Safety of LPG rail transportation: influence of safety barriers

V. Busini*, M. Derudi, R. Rota
Politecnico di Milano, Department of Chemistry, Materials and Chemical Engineering "G. Natta",
Piazza Leonardo da Vinci 32, 20133 Milano, Italy

Abstract: The risk due to the road and rail transportation of liquefied petroleum gas (LPG) is well known. Severe scenarios were caused by road or rail accidents involving LPG pressurized tank cars. Consolidated approaches exist for the analysis, the prevention and the mitigation of risk due to the transportation of hazardous materials (HazMat) by road or rail. In Europe a specific regulation applies to the equipment used for the transport of HazMat and specific regulations apply to the qualification of equipment used for LPG transportation. Nevertheless, on June 29th, 2009, an extremely severe transportation accident involving LPG took place in the station of Viareggio, in Italy. A train carrying 14 tank cars of LPG derailed and several railcars overturned on the shunts in the Viareggio station. A tank was punctured, releasing its entire content that ignited causing an extended and severe flash-fire.
The present study focused on the study of the effect of different parameters on the heavy gas cloud dispersion resulting from the accident, such as meteorological parameters and height of safety walls.
It was found that, to be effective, the mitigation barriers must be carefully designed, with particular reference to their height with respect to the height of the heavy gas cloud.

Keywords: Hazardous Material Transportation, Consequence Analysis, CFD models, Heavy Gas Dispersion Modeling, LPG, Viareggio accident.

1. INTRODUCTION

Accidents involving the release of hazardous substances are a major concern in industrial and transportation risk assessment. They can lead to consequences with high magnitude as the formation of a hazardous cloud can spread over distances of kilometers and pose a risk to both human health and the environment. Urban areas are easily involved in the release of hazardous substances, not only because many industries are part of urban agglomerations as a result of the growth of cities, but also because the transport of substances by road and rail usually crosses the cities. The latter, though usually involves smaller amounts of substances, represents a serious hazard because the accident mitigation is less effective. In addition, the transport vehicles pass near highly vulnerable populated areas such as schools and hospitals. Such accidents in urban areas are therefore a highly dangerous scenario in terms of the magnitude of the consequences, worsen by the high population density present in these areas.
Urban areas are characterized by complex geometries because of the large number of buildings, of various shapes and sizes; these obstacles affect strongly the wind speed and direction because of the presence of trails, stagnant zones, recirculation and preferential pathways which may significantly complicate the scenario.
Accidental releases of hazardous substances have been studied since the '80s and have been investigated through the execution of tests of large spills and the development of numerical models. These models continue to be currently used for the study of the consequences of releases [1, 2], and some of them, such as DEGADIS, ALOHA, and UDM, are among the most widely used in engineering applications [3, 4]. These are lumped parameter models, usually one-dimensional and account for some physical phenomena using semi-empirical relationships whose parameters have been derived from field tests [5]. Since the experimental setup of these tests usually do not involve any obstacle, these models are able to provide reliable results in an open field, or when almost no obstacle occurs in the region covered by the cloud.
To analyze the effects of a multitude of obstacles with different geometries on the dispersion of the cloud, computational tools based on computational fluid dynamics (CFD) are necessary. This approach allows the complete three-dimensional analysis and forecasting velocity, temperature and

*valentina.busini@polimi.it

concentration fields in the domain of integration. Although this procedure may provide more detailed results, it requires a large amount of resources in terms of both computation time and skills of the analysts.
In previous works [6-8], the dispersion of the LPG cloud in Viareggio as it happened in 2009 accident has been simulated using a CFD model; the present work involves the study of the effect of different parameters on the heavy gas cloud dispersion, such as: atmospheric stability class, wind velocity, and presence of mitigation walls of different height.

2. MATERIALS AND METHODS

Computational fluid dynamics codes solve numerically the Navier–Stokes equations of motion (Eqs. (1) and (2)), the energy balance (Eq. 3) and the equation arising from the turbulence modeling [9].

$$\frac{\partial \rho}{\partial t} + \nabla \cdot (\rho \vec{v}) = 0 \qquad (1)$$

$$\frac{\partial (\rho \vec{v})}{\partial t} + \nabla \cdot (\rho \vec{v} \vec{v}) = -\nabla p + \nabla \cdot (\bar{\bar{\tau}}) + \rho \vec{g} \qquad (2)$$

$$\frac{\partial (\rho c_v T)}{\partial t} + \nabla \cdot \left(\rho \vec{v} c_p T\right) = \nabla \cdot (k_T \nabla T) \qquad (3)$$

In the equation above, ρ is the density, t the time, v the velocity, p the pressure, τ the shear stress, g the gravity acceleration, c_v and c_p the specific heats, T the temperature and k_T the thermal conductivity.
In this work the k–ε model was used for representing the effects of the turbulence. This model introduces two additional transport equations for turbulent kinetic energy k (Eq. 4) and turbulent kinetic energy dissipation rate ε (Eq. 5), respectively [10]:

$$\frac{\partial (\rho k)}{\partial t} + \frac{\partial (\rho k v_i)}{\partial x_i} = \frac{\partial}{\partial x_j}\left[\left(\mu + \frac{\mu_t}{\sigma_k}\right)\frac{\partial k}{\partial x_j}\right] + G_k + G_b - \rho\varepsilon - Y_M + S_k \qquad (4)$$

$$\frac{\partial (\rho \varepsilon)}{\partial t} + \frac{\partial (\rho \varepsilon v_i)}{\partial x_i} = \frac{\partial}{\partial x_j}\left[\left(\mu + \frac{\mu_t}{\sigma_\varepsilon}\right)\frac{\partial \varepsilon}{\partial x_j}\right] + C_{\varepsilon 1}\frac{\varepsilon}{k}(G_k + C_{\varepsilon 3}\, G_b) - C_{\varepsilon 2}\rho\frac{\varepsilon^2}{k} + S_\varepsilon \qquad (5)$$

where v_i is the velocity component along x_i direction, μ the viscosity, μ_t the turbulent viscosity, G_k the shear stress-related turbulent kinetic energy production, G_b the buoyancy-related turbulent kinetic energy production, Y_M the compressibility-related kinetic energy production and S_k and S_ε are user-defined source terms. $C_{\varepsilon 1}$, $C_{\varepsilon 2}$, $C_{\varepsilon 3}$, σ_k, σ_ε and C_μ are empirical constants; in this work, Jones and Launder [11] values have been used.
The k–ε turbulence model was complemented with an Atmospheric Stability sub-Model (ASsM) [12], able to ensure the consistency of the CFD results with the Monin-Obukhov theory [8], by introducing a user-defined source term S_ε defined as (for neutral conditions):

$$S_\varepsilon(z) = \rho\frac{u_*^4}{z^2}\left[\frac{(C_{2\varepsilon} - C_{1\varepsilon})\sqrt{C_\mu}}{K^2} - \frac{1}{\sigma_\varepsilon}\right] - \mu\frac{2\,u_*^3}{K\,z^3} \qquad (6)$$

Moreover, for the ground boundary conditions, the ASsM model uses a roughness constant, C_s, equal to 0.979 in the wall functions, and a surface shear stress, τ_w.
The domain is discretized through the use of a calculation grid allowing for transforming the partial differential equations into a system of algebraic equations.
The commercial package Fluent 12.1.2 [13] was used for all the computations, together with the boundary conditions summarized in Table 1.
.

Table 1: Summary of boundary conditions

Boundary	Type	Notes
wind Inlet boundary	velocity inlet	wind velocity, temperature and turbulence values for the wind inlet flux
wind Outlet boundary	pressure outlet	constant pressure outlet surface
top boundary	velocity inlet	wind velocity, tangential to the surface
ground boundary	wall	no slip boundary, roughness specification, fixed temperature; gas mass fraction was specified in the region of the pool
buildings walls	wall	flat and adiabatic
gas inlet boundary	mass flow inlet	mass flow, temperature and turbulence values for the gas flux

3. RESULTS

The meteorological condition at the moment of the accident in Viareggio were: stable class (F), wind speed 0.7 m/s, direction E-SE; the final footprint of LPG cloud, that is at 300 s after the release, is sketched in Figure 1 for the sake of comparison. For further details and for the comparison with the field evidences the readers can refer to previous works [6-8]. Because of the agreement found with the field evidences, we will refer in the following to this case as the "real case".

Figure 1: LFL (black) and UFL (red) footprints at 300 seconds

In this work, a neutral stability class with wind velocity of 5 m/s at 10 m (5D) was considered with two different wind directions: the actual wind direction of the Viareggio accident (E-SE) and the opposite one (W-NW). For these two wind direction three different domains were considered: the first one represents the domain of Viareggio as it was the day of the accident; the second one is the first one with a wall 2.5 m high on the east side of the station added; in the third domain two continuous walls 4.5 m high on both sides of the station (east and west) were added.

3.1. The real case with different atmospheric conditions

The results in Figure 2 are relative to the case with the actual wind direction of the Viareggio accident (E-SE) and show how a higher wind velocity, with respect to the real case shown in Figure 1, entails a higher dispersion of the LPG leading to a different and less widespread footprint of the cloud. The figure also shows that no upwind spreading of the cloud is present in this case: therefore, less houses are involved and they are located only on the east side.

Figure 2: LFL (black) and UFL (red) footprints at 180 and 300 seconds for 5D E-SE atmospheric conditions

Figure 3, which is relative to the case with wind direction W-NW, shows how the already existing walls on the west side (2.3 meters high) are able to contain the cloud. Contrary to the previous case, we can see that the cloud extends only to the west side.

Figure 3: LFL (black) and UFL (red) footprints at 180 and 300 seconds for 5D W- SW atmospheric conditions

3.2 The case with 2.5 m high mitigation wall on the east side

Successively, a configuration with a mitigation wall 2.5 m high added on the east side was investigated. As evident from the results summarized in Figure 4, this mitigation wall is not able to contain completely the cloud that extends to the first to rows of houses.

Figure 4: LFL (black) and UFL (red) footprints at 180 and 300 seconds for 5D E-NE atmospheric conditions and a wall 2.5 m high on the east side

The simulation performed for the W-SW wind direction (Figure 5) resulted in a footprint similar to that shown in Figure 3.

Figure 5 LFL (black) and UFL (red) footprints at 180 and 300 seconds for 5D W-SW wind atmospheric conditions and a wall 2.5 m high on the east side

The different behaviours of the cloud in the last two cases, that is the wall on the west side is effective while the one on the east side even though with the same height is not, arise from a canalization of the wind in the latter case, as shown in Figure 6.

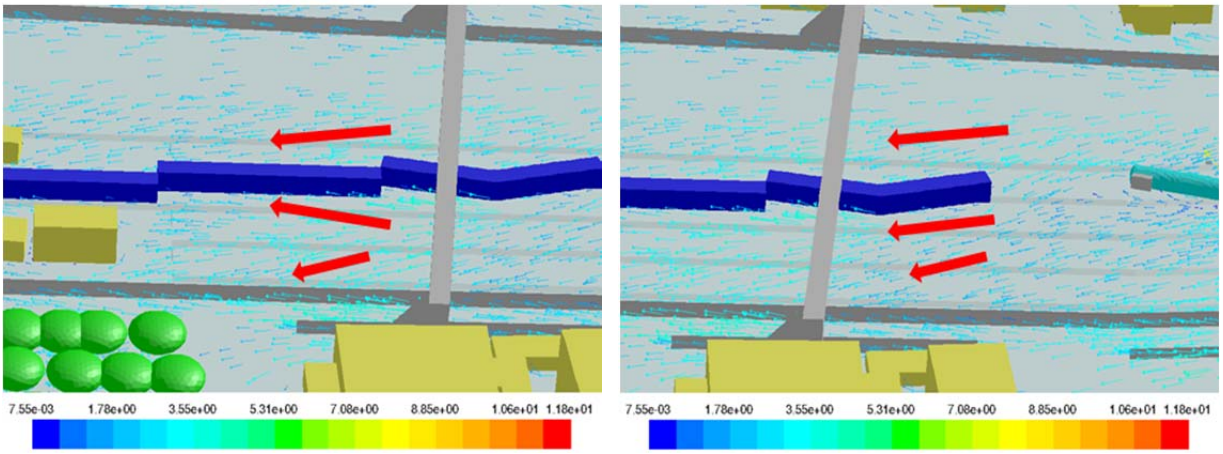

Figure 6: Velocity vectors along the train (left) and near the punctured tank (right) at 1 meter above the ground

We can see that the cloud is divided into two parts by rail tankers and thus channelled along the tracks following the line of rail tank cars; in this way a smaller portion of the cloud gets to the west wall.

3.2 The case with 4.5 m high mitigation walls on both sides

In the last configuration considered, a wall of 4.5 m was added on both sides. The height was chosen on the bases of the general criterion that a mitigation wall is effective in reducing the hazardous distance from a cloud dispersion when its height is comparable to that the cloud reaches without the mitigation wall [14]. Figure 7 shows that the height of the cloud in proximity of the mitigation wall position is about 4.5 m (as computed from the absolute height reported in the figure minus the altitude of Viareggio, which is equal to about 2.5 m on the sea level).

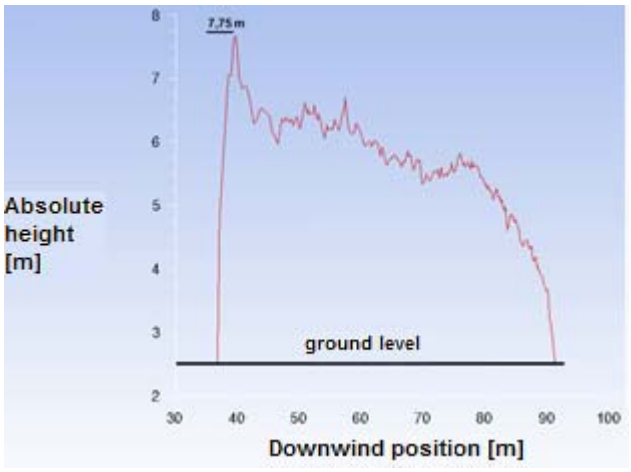

Figure 7: Downwind cloud height

With the presence of these walls, the cloud can be confined both on the east side (Figure 8) and on the west side (Figure 9).

Figure 8: LFL (black) and UFL (red) footprints at 180 and 300 seconds for 5D E-NE atmospheric conditions and two walls 4.5 m high on both sides

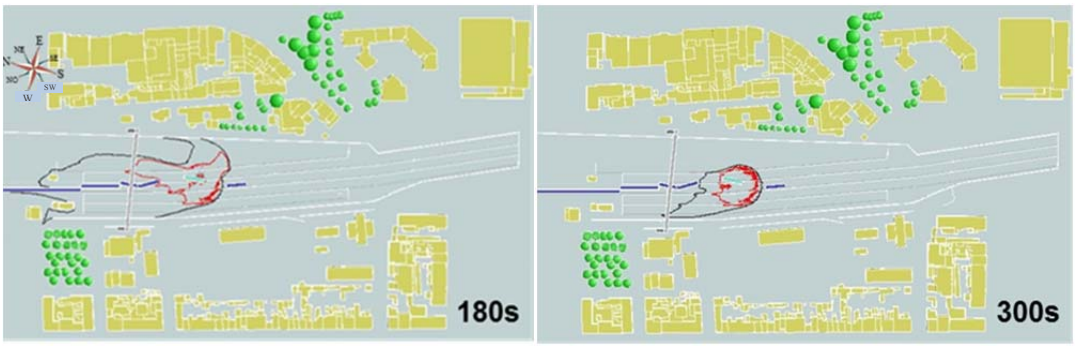

Figure 9: LFL (black) and UFL (red) footprints at 180 and 300 seconds for 5D W-SW atmospheric conditions and two walls 4.5 m high on both sides

Figure 9 also shows a peculiar behavior of the cloud footprint in the sketch at 180 s: the 4.5 m additional wall on the east side creates a special situation leading to the formation of a concentration area with the shape of "lagoon" near to the east wall. This behavior can be explained analyzing the velocity vectors on the ground and at 1 m height (Figure 10): they show that the wind has two main direction, one along the train and another along the wall.

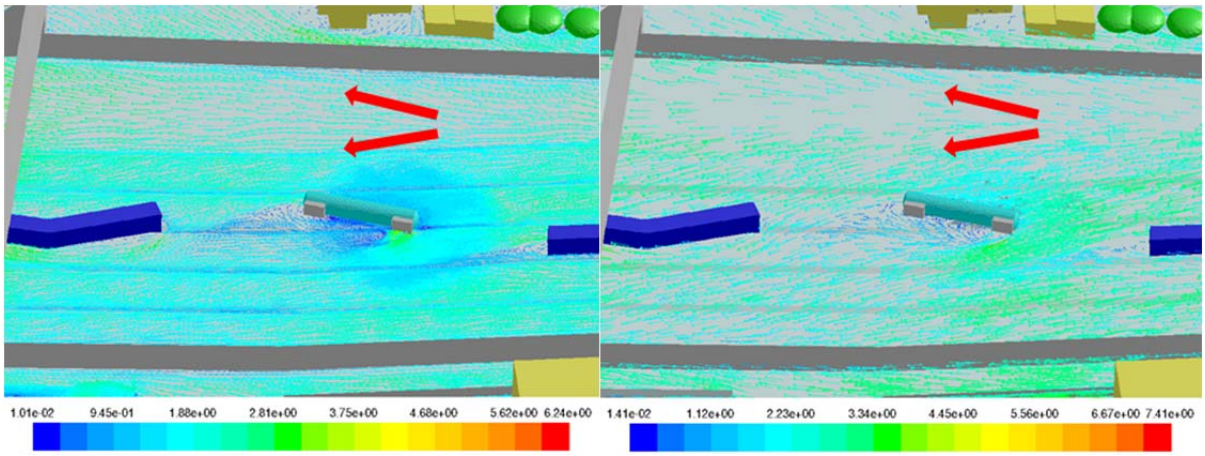

Figure 10: Velocity vectors at ground level (left) and 1 meter above the ground (right)

4. CONCLUSION

This work was aimed at studying the effect of different atmospheric conditions as well as the effectiveness of mitigation barriers of various heights on the dispersion of clouds produced by the release of LPG in urban areas.
As expected, a higher wind velocity together with a neutral atmospheric stability class entails a higher dispersion of the LPG leading to a different and less widespread footprint of the cloud, while the effect of introducing mitigation barriers is harder to predict.
The examined case studies derived from the real case of the accident of Viareggio considering two wind directions in three different geometrical domains: the first one represents the domain of Viareggio as it was the day of the accident, the second one is the same domain with a wall 2.5 m high on the east side of the railway station, while the third domain involves two continuous mitigation walls 4.5 m high on both sides of the railway station (namely, east and west sides). It has been found that in all the domains with the E-NE wind direction the cloud bypasses the mitigation barriers, while for the W-SW wind direction the cloud is always contained by the mitigation barriers thanks to a channeling of the cloud along the track.
These results clearly indicate the importance of carefully investigating through CFD tools the effect of introducing a mitigation barrier.

References

[1] M. Nielsen and S. Ott. "*A collection of data from dense gas experiments*", (1996).

[2] S. R. Hanna and R. E. Britter. "*Wind Flow and Vapor Cloud Dispersion at Industrial and Urban Sites*". 2002.

[3] A. Bernatik and M. Libisova. "*Loss prevention in heavy industry: risk assessment of large gasholders*", Journal of Loss Prevention in the Process Industries,17:271-278, (2004).

[4] D. R. Brook, N. V. Felton, C. M. Clem, D. C. H. Strickland, I. H. Griffiths and R. D. Kingdon. "*Validation of the Urban Dispersion Model (UDM)*", International Journal of Environment and Pollution,20:11-21, (2003).

[5] M. Fingas. "*The Handbook of Hazardous Materials Spills Technology*". 2002.

[6] V. Busini, M. Pontiggia, M. Derudi, G. Landucci, V. Cozzani and R. Rota. "*Safety of LPG Rail Transportation*", Icheap-10: 10th International Conference on Chemical and Process Engineering, Pts 1-3,24:1321-1326, (2011).

[7] G. Landucci, A. Tugnoli, V. Busini, M. Derudi, R. Rota and V. Cozzani. "*The Viareggio LPG accident: Lessons learnt*", Journal of Loss Prevention in the Process Industries,24:466-476, (2011).

[8] M. Pontiggia, G. Landucci, V. Busini, M. Derudi, M. Alba, M. Scaioni, S. Bonvicini, V. Cozzani and R. Rota. "*CFD model simulation of LPG dispersion in urban areas*", Atmospheric Environment,45:3913-3923, (2011).

[9] A. Luketa-Hanlin, R. P. Koopman and D. L. Ermak. "*On the application of computational fluid dynamics codes for liquefied natural gas dispersion*", Journal of Hazardous Materials,140, (2007).

[10] M. Pontiggia, M. Derudi, M. Alba, M. Scaioni and R. Rota. "*Hazardous gas releases in urban areas: Assessment of consequences through CFD modelling*", Journal of Hazardous Materials,176:589-596, (2010).

[11] G. S. W. Hagler, M. Y. Lin, A. Khlystov, R. W. Baldauf, V. Isakov, J. Faircloth and L. E. Jackson. "*Field investigation of roadside vegetative and structural barrier impact on near-road ultrafine particle concentrations under a variety of wind conditions*", Science of the Total Environment,419:7-15, (2012).

[12] V. Busini, M. Lino and R. Rota. "*Influence of Large Obstacles and Mitigation Barriers on Heavy Gas Cloud Dispersion: a Liquefied Natural Gas Case-Study*", Industrial & Engineering Chemistry Research,51:7643-7650, (2012).

[13] ANSYS Inc. ANSYS Fluent 12 User's guide. 2009.

[14] M. Derudi, D. Bovolenta, V. Busini and R. Rota. "*Heavy gas dispersion in presence of large obstacles: selection of modeling tools*", Industrial & Engineering Chemistry Research (10.1021/ie4034895).